

Low Cycle Fatigue of Precipitation Hardened Aluminum Alloy

Dr. Dhafir S. Al-Fattal

Machines and Equipment Engineering Department, University of Technology/ Baghdad

Saif Khalid Mahmood

Machines and Equipment Engineering Department, University of Technology/ Baghdad

Email: saifkhalid00@yahoo.com

Received on:28/8/2014 & Accepted on:8/10/2015

ABSTRACT

In this work, the influence of different heat treatments on the mechanical properties and fatigue life under low cycles of wrought 7075 aluminum alloy was experimentally investigated. The heat treatments included peak ageing (T6), over ageing (T73) and annealing (O). The flat fatigue specimens were subjected to constant reverse bending load. The tests were performed at the laboratory environment with a frequency of 23.6 Hz and at a stress ratio (R) of -1. For each temper, strain-life graphs were obtained for specimens with notches in the form of central cylindrical holes made by drilling. The fatigue resistance of specimens with notches was compared to the results for notch-free specimens. It was observed that the presence of a stress raiser, such as a drilled hole, lowers the fatigue life for all tempers. However, the notch sensitivity of the fatigue life was different for each temper. The fatigue crack growth rate of T73 and annealed temper was investigated; the results showed that T73 treated sample exhibits higher crack growth resistance. Paris' equation was derived for each temper.

Keywords: Precipitation Hardening, Low Cycle Fatigue, 7075 AL-Alloy, Fatigue Crack Growth.

كلال الدورات المنخفضة في سبيكة الألمنيوم قابلة للتصليد بالترسيب

الخلاصة

في هذا البحث، تم التحقق عملياً من تأثير معاملات حرارية مختلفة على الخواص الميكانيكية وعلى عمر الكلال تحت دورات منخفضة لسبيكة الألمنيوم 7075. تضمنت المعاملات الحرارية: التعتيق لاقصى صلادة (T6) والتعتيق المفرط (Overageing, T73) والتخمير (O). تعرضت عينة الكلال المسطحة الى حمل انحناء متعاكس ثابت السعة. تم اجراء الاختبار في جو المختبر مع تردد 23.6 Hz ونسبة اجهاد -1. لكل معاملة حرارية، تم ايجاد منحنيات الانفعال- العمر لعينات ذات حوز بشكل ثقوب اسطوانية مركزية صنعت بعملية التثقيب. تم مقارنة مقاومة الكلال للعينات المحززة مع نتائج مقاومة الكلال لعينات غير محززة. لوحظ ان وجود رافعات الاجهاد، كما الحال في الثقوب، تخفض عمر الكلال لكل المعاملات، ولكن كان تأثير حساسية الحز على عمر الكلال مختلف لكل معاملة. تم التحقق من معدل نمو الشق لمعاملة التخمير و معاملة T73 و اظهرت النتائج ان معاملة T73 لها مقاومة اعلى لنمو الشق. تم ايجاد معادلة باريس لكل معاملة.

INTRODUCTION

Aluminum and its alloys are used in a variety of cast and wrought forms and conditions of heat treatment. For over 70 years, it ranks next to iron and steel in the metal market. The demand for aluminum grows rapidly because of its unique combination of properties which makes it become one of the most versatile of engineering and construction material [1]. The optimum properties of aluminum are achieved by alloying additions and heat treatments. This promotes the formation of small hard precipitates which interfere with the motion of dislocations and improve its mechanical properties [2]. One of the most commonly used aluminum alloy for structural applications is 7075 Al alloy due to its attractive comprehensive properties such as low density, high strength, ductility, toughness and resistance to fatigue [3]. It has been extensively utilized in aircraft structural parts and other highly stressed structural applications [4].

One of the essential goals in the fatigue process study is the prediction of the fatigue life of a structure or machine component subjected to a given stress–time history. To allow this prediction, complete information about the response and behavior of the material subjected to cyclic loading is necessary. In addition to the characterization of the cyclic stress–strain response, quantitative information on resistance to crack initiation and growth are of primary importance [5]. The objective of the current work is to investigate the effect of heat treatment on the mechanical properties and LCF behavior of 7075 aluminum alloy.

Experimental Procedure

Material used in this study is a sheet of AA 7075 aluminum alloy (bare product). Chemical analysis of the alloy was carried out by Thermo ARL 3460, optical Emission spectrometer. The results are summarized in Table 1.

Table (1): Chemical composition of the alloy.

Element	Fe%	Cu%	Mn%	Mg%	Cr%	Zn%	Al%
	0.238	1.81	0.010	2.14	0.182	5.52	Bal.

Heat Treatment

In addition to the treatment of the as-received material (T73 temper), two other tempers were achieved. All the following heat treatment processes were done according to ASTM standard (B 918 – 01):

- **annealing (full annealing):** The specimens were heated to 415°C for 2.5 hr then cooled in still air at an uncontrolled rate to 195°C followed by reheating to 230°C ± 3°C for 4 hr and cooling in still air.
- **Peak artificial ageing (T6):** Before achieving this treatment, the specimens were annealed to remove the effect of the received temper. Then, they were heated to 480°C ± 4°C for 40 min, quenched in water, and then heated to 120°C ± 3 for 24 hours.

Hardness test

A Vicker’s hardness testing machine type TH714 was used under applied load 4.903N (0.5 kgf) for 15 second on the polished specimen.

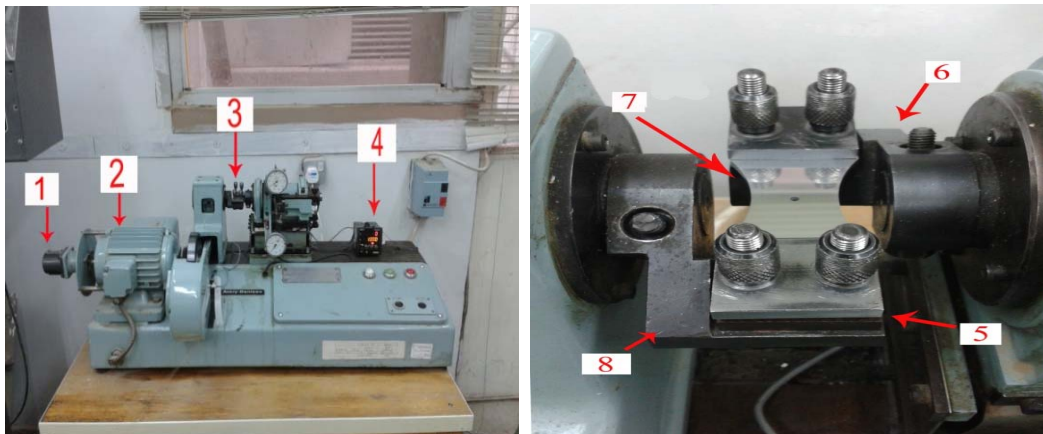
Tensile test

The tensile specimen was prepared according to ASTM with designation B 557 – 02a. From this standard, the total length of the specimen was 200 cm. The tensile test was performed using an (WDW-2000E III) testing machine. The test was achieved with a cross-head speed of 1 mm/min.

Fatigue test

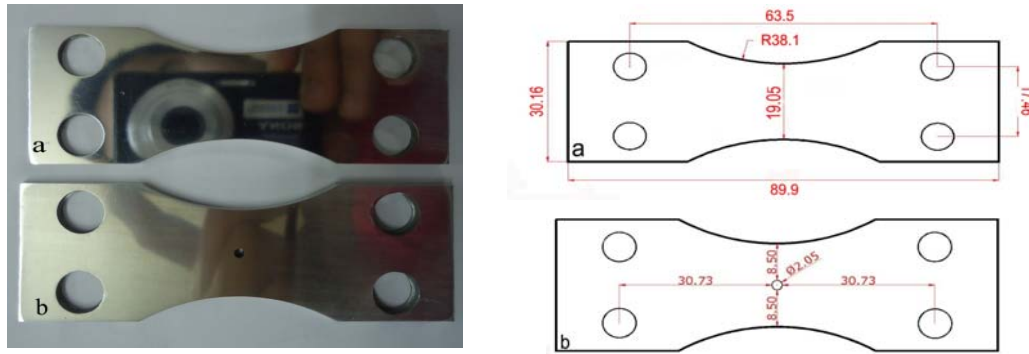
A reverse bending fatigue machine type AVERY DENISON-7306 was used to carry out the fatigue testing, as shown in Fig. 1.

The tests were undertaken in stress control with a stress ratio $R=-1$ and the cycling rate is 1420 rpm ($f=23.6$ Hz). All the tests were performed in the Central Organization for Standardization and Quality Control (C.O.S.Q.C.). For each heat treatment condition, two types of fatigue specimens were tested; the first type, the specimens were cut in suitable dimensions to satisfy the machine test (according to Users’ Instructions Manual). Fig.2a shows the shape and dimensions of fatigue specimens. The second one was includes an additional central drilled hole with 2.05 mm diameter, as shown in Fig. 2b



1. Mechanical counter 2. Motor 3.Specimen fixture 4.Digital counter 5.Clamp
6.Fixed grip 7.The specimen 8.Movable grip

Figure (1) : Fatigue testing machine



(a) Without a hole and (b) with a hole
 Figure (2): Fatigue test specimens (dimensions in mm)

Results and Discussions

The tensile test results are present in Table 2. The results were compatible with standard value [6]. It shows that T6 has the highest strength, this could be due to the heating process to a sufficiently high temperature which leads to few alloying elements (Zn and Mg in this alloy) to dissolve and form a supersaturated solid solution. Subsequent quenching to room temperature freezes the alloying elements in solution. On reheating to an intermediate temperature, the host metal (aluminum) rejects the alloying element in the form of a fine, uniformly distributed precipitates in an aluminum alloy matrix. These fine precipitated particles act as barriers to the motion of dislocations and provide resistance to slip, thereby increasing the strength [7]. It can be also observed that T73 has strength lower than T6. The reason for this is that the precipitation heat-treating temperature used to produce T73 temper is generally higher than that used to produce T6 temper. This leads to over aging and rapid growth of the precipitates and formation of dislocation loops around them which indicates that the precipitates have lost coherency along their boundaries and a new intermediate phase is formed. This carries the mechanical properties beyond the point of maximum strength to provide some special characteristic, such as enhanced resistance to stress-corrosion cracking or to exfoliation corrosion [8].

Table (2): Engineering tensile properties of different tempers.

	Tensile Strength (MPa)	Yield Strength* (MPa)	σ_u/σ_y	El** %
AA 7075-T6	560	490	1.14	11.6
AA 7075-T73	504.71	435	1.16	12.5
AA 7075-O	245.6	107	2.28	16.4

* 0.2 % offset

** In 50 mm (2 in.)

The annealed condition has the lowest strength, but it also has the highest elongation percentage. The dislocation density within the interior of the subgrains decreases during the recovery process. The energy of a boundary increases with misorientation, but

the energy per dislocation decreases with misorientation, i.e., there is a driving force to form fewer and more misoriented boundaries. In recrystallization, nucleation and growth of new dislocation free grains take place at the expense of the deformed microstructure. This makes deformation and dislocation slip faster [9]. The annealing condition has the highest percentage elongation followed by over-aged (T73) and peak-aged samples. This is partly due to grain coarsening which leads to an increase in the grain boundary area which increases the amount of energy required for the movement of dislocations required to cause fracture [10]. Thus, the material can withstand a higher plastic deformation before the final fracture. However, the percentage elongation of T6 condition is small because of embrittlement of 7075 Al alloy as a result of microsegregation of MgZn₂ [11].

The strain hardening exponent (n) and the strength coefficient (k) values were summarized in Table 3. It shows that the (n) value for the O-condition more than of the T73-condition, followed by the T6-condition, while the (k) value for O-condition was less than the other conditions, this means the high movement dislocation that produced from internal strain about precipitation atoms was occurred, and provide more grain boundaries to prevent crack propagation in T73 and T6 conditions [12].

Table (3): Values of k and n for three conditions

	<i>N</i>	K (MPa)
T6	0.144	857.34
T73	0.17	821.29
O	0.37	620.7

Table 4 shows the Vickers hardness of the all conditions in this work. The results showed that T6 temper has the highest hardness value, where aluminum-zinc alloy is susceptible to embrittlement because of microsegregation of MgZn₂ precipitates which serve as foreign atoms or inclusions in the lattice of the host crystal in the solid solution; this causes more lattice distortions which make the alloy harder. In the previous study, solid solution strengthening from elastic distortions is produced by substitutional atoms of Mg and Zn in aluminum matrix [13]. Hence, the main strengthening mechanism in these alloys is precipitation hardening by structural precipitates of MgZn₂ formed during artificial ageing. The precipitate particles act as obstacles to dislocation movement and thereby strengthen the heat-treated alloys. That may lead to catastrophic failure of components produced from it [11].

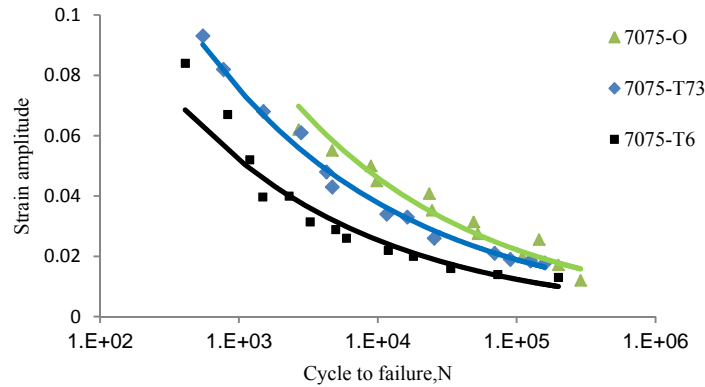
The annealed condition has the lowest hardness. This is due to the high diffusion rates that exist during soaking and slow cooling which permit maximum coalescence of precipitate particles and result in minimum hardness [8].

Table (4): Vickers hardness values.

	HV (kgf/mm²)
AA 7075-T73	149.5
AA 7075-O	70.2
AA 7075-T6	174.9

Low Cycle Fatigue Strength

Fig. 3 depicts the total strain amplitude versus life for alloy AA 7075 at T6, T73 and O-condition. In general, low cycle fatigue life is sensitive to strain amplitude, and the fatigue life decreases as the strain amplitude increases.



Figure(3): Fatigue resistance of 7075 alloy for different tempers.

It can be noted from Fig. 3 that with fatigue life up to 10⁵cycles, the annealed condition has the highest fatigue resistance followed by T73 condition, while T6 has the lowest fatigue resistance.

The behavior of AA 7075 with its three conditions can be predicted numerically as shown in Fig. 4 using Coffin- Manson Eq. to specify fatigue life equations for the three conditions:

For AA 7075-T6; $\frac{\Delta\epsilon_p}{2} = 3.43 (N_f)^{-0.794}$... (1)

For AA 7075-T73; $\frac{\Delta\epsilon_p}{2} = 5.42 (N_f)^{-0.73}$... (2)

For AA 7075-O; $\frac{\Delta\epsilon_p}{2} = 0.887 (N_f)^{-0.35}$... (3)

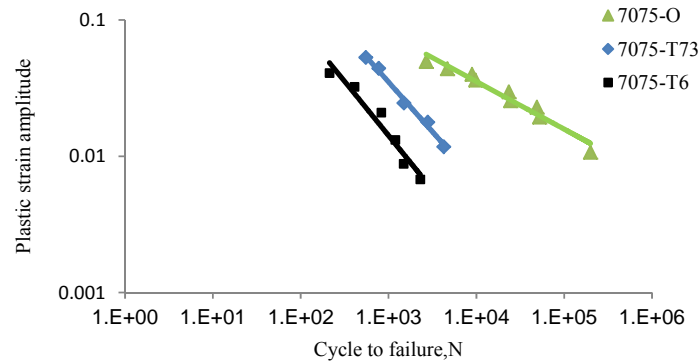


Figure (4): Plastic strain life curve for different tempers.

Fatigue properties obtained from this investigation are compared with the results of previously published researches as listed in Table 5.

Table (5): Comparisons of fatigue properties with previous published researches.

Temper	ϵ'_f	c
T6 [14]	0.12	-0.75
T6 [15]	2.57	-0.9
7075-T6 [This work]	3.433	-0.794
T651 [15]	0.26	0.8-
T651 [16]	0.029	-0.169
T7351 [15]	6.81	-1.19
7075-T73 [This work]	5.42	-0.73
7075-T73 [17]	0.26	-0.73
7075-O [This work]	0.887	-0.35

The variations observed in Coffin-Manson constant (c) are more acceptable than those of the previously published shown in the Table 5. The constant ϵ'_f compares well with similar type of alloys in the table and dose not correlate well with the true fracture ductility in a monotonic tensile test. The same results and conclusions were presented by Meggiolaro and Castro [14].

Effect of drilled hole on low cycle fatigue strength

Figs. 5 to 8 illustrate the fatigue behavior of drilled specimen. The results revealed that the effect of hole on the fatigue strength of all tempers is different. The highest effect is observed in the annealed condition, followed by T73 and T6.

Approximately, at 10^4 cycles, there is a remarkable shift in the behavior of the alloy in the T73 and O conditions. Above this transition, it is clear that T73 condition tolerates more cycles to failure at the same strain compared to the annealed condition, as shown in Fig. 8.

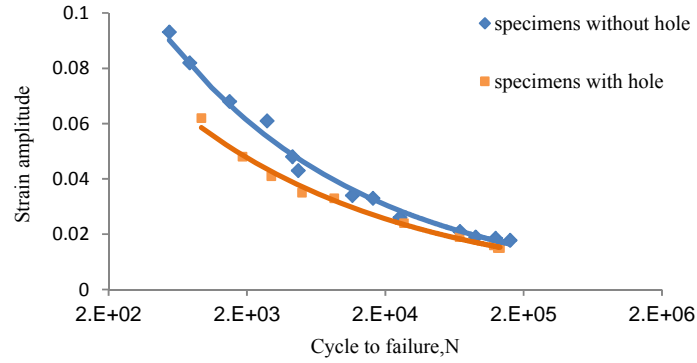
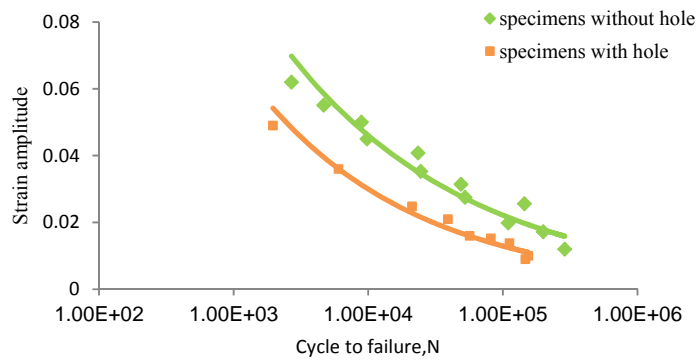


Figure (5): Effect of hole on 7075-T73 alloy.



Figure(6): Effect of hole on 7075-O alloy.

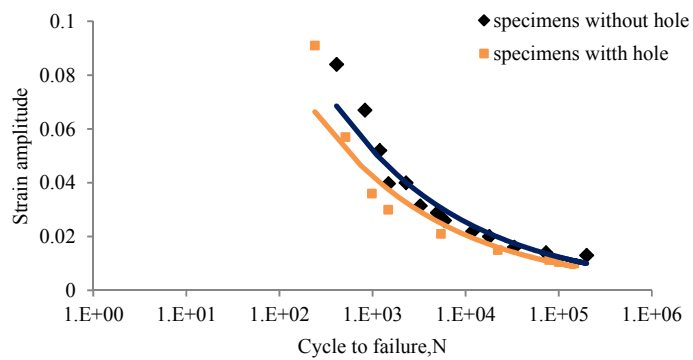


Figure (7): Effect of hole on 7075-T6 alloy.

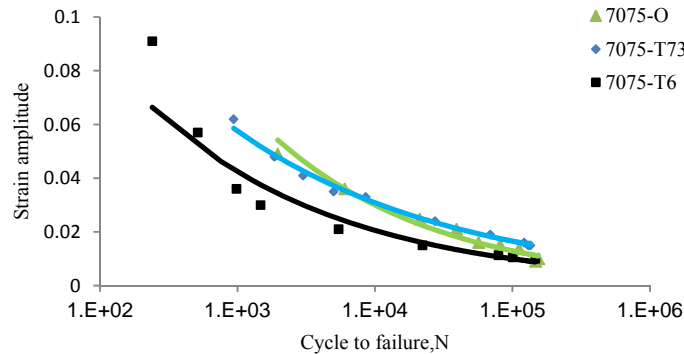


Figure (8): Total strain life curve of drilled specimens.

Fatigue Crack Growth Modeling

The fatigue crack growth study was conducted on T73 temper and annealed condition (samples with a central cylindrical hole). The specimens were subjected to a constant loading with frequency of 23.6 Hz and at a stress ratio (R) of -1.

To study the crack growth behavior, crack extension vs. number of stress cycle plots were generated, and slopes at different crack lengths were calculated, see Figs. 9 and 10. To illustrate the crack growth behavior, the slope of the curve, da/dN , i.e, fatigue crack growth rate (FCGR), is plotted as a function of stress intensity range (ΔK) as shown in Fig. 11. ΔK values were calculated from the average crack length of

two successive crack length measurements. The compressive half cycles of fatigue was omitted in the calculation of ΔK .

The initiation sites were generally from the left and right edge of the hole. Initially, more than one crack were initiated, but after that one of them became the main crack and led to failure.

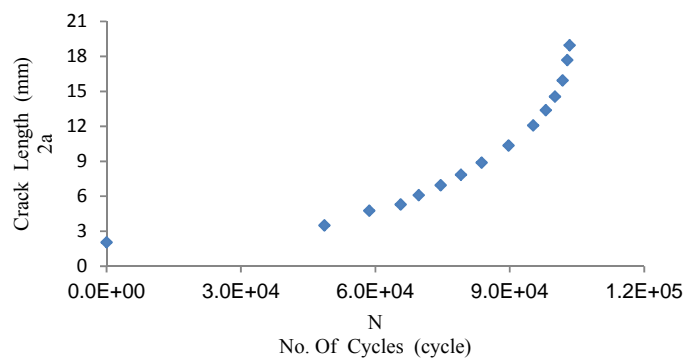


Figure (9): Fatigue crack propagation of 7075-T73.

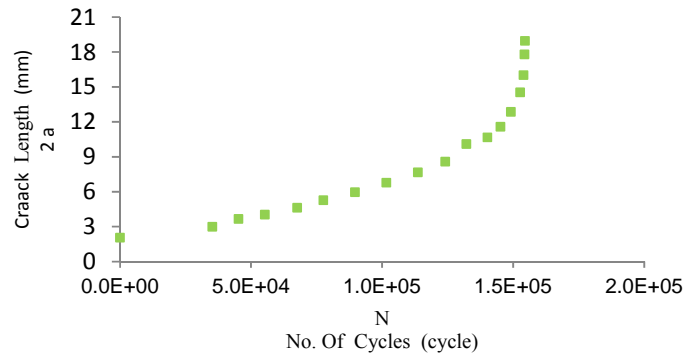


Figure (10): Fatigue crack propagation of 7075-O.

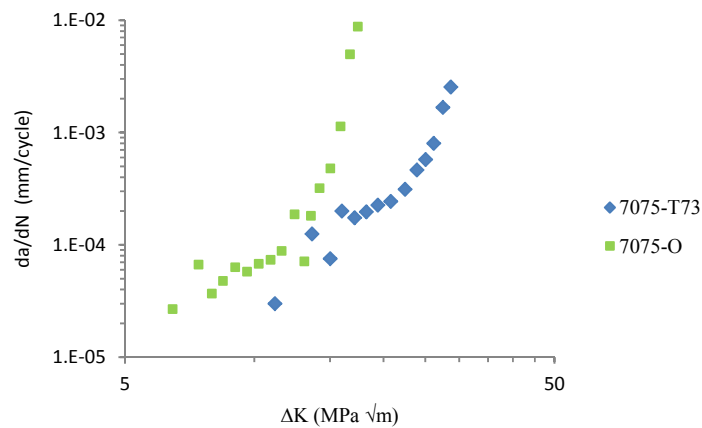


Figure (11): Fatigue crack growth rate for the alloy in two different heat treatments.

The trend of the results shows that the fatigue threshold for crack growth (ΔK_{th}) of overaged temper is expected to be higher than that of the annealed condition. The results also showed that the T73 overaged sample exhibited lower crack growth rate than the annealed sample.

The present results of crack growth can be explained on the basis of the microstructures. According to the works by Hornbogen and Zum Gahr [18], the shearable precipitates may promote a planar dislocation distribution. When a cyclic loading is applied, a certain number of dislocations are able to move backwards during unloading on the same slip plane during the forward motion in the rising part of a loading cycle. Some of these dislocations therefore leave the material at the crack tip and thus do not contribute to crack growth. For the non-shearable precipitates, however, the dislocations have to bypass them during the rising part of the loading cycle. It is hard for the dislocations to move backwards on the original slip plane

during unloading. Therefore, a large number of dislocations will be concentrated at the crack tip, which would result in a high crack growth rate. The microstructures of T73 temper has finer and more coherency precipitates with the Al matrix than annealed condition, so these precipitates are mainly sheared by the dislocations, promoting planar slip and enhancing the reversibility of dislocation motion. Therefore, the fatigue crack growth rate of T73 treated sample is lower than annealed temper.

To obtain Paris equations for each temper (the values of C and m), a least-square method can usually be adopted to fit the fatigue data. This linear portion of the curve in the log-log scale plot of da/dN as a function of ΔK, as shown in Fig. 12.

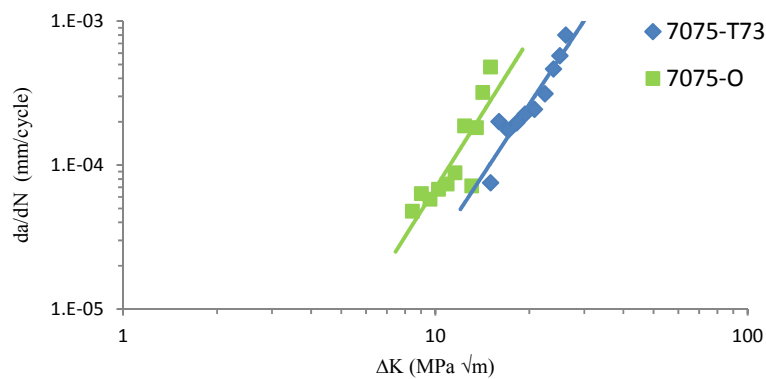


Figure (12): The relation between crack growth rate and the stress intensity factor range for 7075-T73 and 7075-O

Paris equation for 7075-T73; $\frac{da}{dN} = 1.321 * 10^{-8} * \Delta k^{3.307}$... (4)

Paris equation for 7075-O; $\frac{da}{dN} = 2.415 * 10^{-8} * \Delta k^{3.455}$... (5)

Fig. 12 shows the difference between 7075-T73 and 7075-O for the fatigue crack growth in Paris region. It can be observed that the annealed condition has a faster crack growth rate at the same stress intensity factor range (ΔK) level

CONCLUSIONS

1. As compared with the received temper (T73), T6 treatment enhanced the strength by 10.9% and reduced the elongation by 7.2%. In the annealed condition, the strength was reduced and the elongation was improved by 51.33% and 31.2%, respectively.
2. The annealed condition has the highest value of n, while T6 has the lowest.
3. The annealed condition has the highest ability for strain hardening followed by over ageing and peak ageing temper.
4. The effect of hole on fatigue strength of all tempers is different. The highest effect was observed in the annealed condition followed by T73 and T6.

5. T73 treated sample exhibited higher crack growth resistance than annealed condition

REFERENCES

- [1].American Society for Metals, “Properties and Selection. Nonferrous Alloys and Special-Purpose Materials”, ASM International Handbook Committee, 1990.
- [2].Smallman RE.,” Modern Physical Metallurgy. 4th ed.”, London, Butterworths and Co., 1985.
- [3].Heinz A and Haszler A., “Recent Development in Aluminum Alloys for Aerospace Applications”, Materials Science and Engineering, Vol. 280, Issue 1, pp. (102-107), 2000.
- [4].Zhao T and Jiang Y., “Fatigue of 7075-T651 Aluminum Alloy”, International Journal of Fatigue, Vol. 30, Issue 5, pp. (834-849), 2008.
- [5].L.P. Borrego, L.M. Abreu, J.M. Costa, and J.M. Ferreira, “Analysis of Low Cycle Fatigue in AlMgSi Aluminum Alloys”, Engineering Failure Analysis, Vol. 11, Issue 5, pp.(715–725), 2004.
- [6].ASM International, Vol.2, “Properties and Selection: Nonferrous Alloys and Special-Purpose Materials”, 1990
- [7].Arkan J. Abassa, Dhafer S. Al-Fatal, “Experimental and Theoretical Study of The Influence of The Addition of Alumina Powder to 7020 Aluminum Alloy Foam on The Mechanical Behavior Under Impact Loading”, IJMET, Vol. 3, Issue 3, pp. (412-428), 2012.
- [8].ASM International, Vol.4, “Heat Treating”, 1991.
- [9].Humpherys, F.J., and Hartherly, M., “Recrystallisation and Related Annealing Phenomena”, Pergamon Press, Oxford, 1995.
- [10].Liao X Z, Zhao Y H and Zhu YT, “Grain-size Effect on The Deformation Mechanisms of Nanostructured Copper Processed by High-Pressure Torsion”, Journal of Applied Physics, Vol.96, No.1, pp. (636-640), 2004.
- [11].Adeyemi D. I sadare, Bolaji A., Mosobalaje O. Adeoye, Oluyemi J. Olawale, and Moshood D. Shittu, “ Effect of Heat Treatment on Some Mechanical Properties of 7075 Aluminum Alloy”, Materials Research, Vol.16, pp. (190-194), 2013.
- [12].Haji, Z. N., “Low cycle fatigue behavior of aluminum alloys AA2024-T6 and AA7020-T6”, Diyala Journal of Engineering Sciences, Vol.0, No. 0, pp. (127-137), 2010.
- [13].Zhao YH, Liao XZ, Jin Z, Valiev RZ and Zhu YT. “Microstructures and Mechanical Properties of Ultrafine Grained 7075 Al alloy Processed ECAP and Their Evolutions During Annealing”, Acta Materialia, Vol.52, Issue 15, pp. (4589–4599), 2004.
- [14].M.A. Meggiolaro, and J. T. P. Castro, “Statistical Evaluation of Strain-Life Fatigue Crack Initiation Predictions”, International Journal of Fatigue, Vol. 26, Issue 5, pp. (463–476), 2004.
- [15].A. Fatemi, A. Plaseied, A.K. Khosrovaneh , and D. Tanner, “Application of bi-Linear log–log S–N Model to Strain-Controlled Fatigue Data of Aluminum Alloys and Its Effect on Life Predictions”, International Journal of Fatigue, Vol. 27, Issue 9, pp. (1040–1050), 2005.

- [16].E. U. Lee, A. K. Vasudevan, and G. Glinka, “Environmental Effects on Low Cycle Fatigue of 2024-T351 and 7075-T651 Aluminum Alloys”, *International Journal of Fatigue*, Vol. 31, Issues 11–12, pp. (1938–1942), 2008.
- [17].M. Benachour, N. Benachour, and M. Benguediab , “Fatigue Crack Initiation of Al-Alloys-Effect of Heat Treatment Condition”, *International Science Index*, Vol.13, pp. (757-759), 2013
- [18].Hornbogen E and Zum Gahr K H. “Microstructure and Fatigue Crack Growth in Fe-Ni-Al Alloy”. *Acta Metallurgica*, Vol. 24, Issue 6, pp. (581–592), 1976.